SEISMIC TESTS OF SLAB - COLUMN CONNECTIONS OF FLAT PLATE CONSTRUCTION USING HIGH STRENGTH CONCRETE

Hyong-Kee KIM[1], Fumitoshi KUMAZAWA[2], Yoshiaki NAKANO[3] and Tsuneo OKADA[4]

1. INTRODUCTIONS

A flat plate construction is one of the R/C structural systems consisting of plane slabs supported directly on columns without any capitals. This construction system has an advantage of flexibility for architectural design because no beams are required for structural elements.

Since the use of high strength concrete recently has become in practice for reinforced concrete structures, it is highly desired to establish the seismic design method for flat plate construction using high strength concrete under the present condition that the seismic design method does not exist in high strength concrete, while exists in normal strength concrete.

The objectives of this study are (1) to investigate the applicability of design formulas which is commonly used in designing R/C flat plate structures to the case of using high strength concrete and (2) to obtain the fundamental data in order to establish the seismic design method for flat plate construction using high strength concrete.

In this paper, interior slab-column subassemblages constructed with high strength concrete were tested under simulated seismic and gravity loads to evaluate their strength and behavior. The test parameters were slab reinforcement ratios and the gravity load levels.

2. TEST METHOD

2.1 TEST SPECIMEN

Test specimens were 1/2.5 scaled models of interior slab-column connection parts of flat plate construction. The number of specimens was four with the test parameters summarized in Table. 1, and the details are shown in Fig. 1. The modeling and boundary conditions of the specimens were based on the assumption that points of inflection in the prototype building under lateral loading are at mid spans and mid-stories. Each specimen consisted of 25 cm × 25 cm columns and a 250 cm × 280 cm slab with 10 cm thickness.

Two types of slab reinforcing bar arrangement were consisted in the specimens; one corresponded to the prototype model based on the current design method in Japan, and the other had twice reinforcing bar approximately in order to lead the specimen to punching shear failure without flexural failure and then

---

[1] Graduate Student, University of Tokyo

[2] Research Associate, Institute of Industrial Science, University of Tokyo

[3] Associate Professor, ditto

[4] Professor, ditto

investigate the punching shear strength for connection transferring both the moment and the shear. In the case of the specimens; FPS01, FPS02 and FPS04 corresponding to the prototype model, the slab top reinforcement ratio of the column strip was 0.59%, and the ratio in the other part was half as much. In the case of the specimen; FPS03, the slab reinforcement ratio of the column strip was 1.10%, and the other part was also half as much.

Mechanical properties of concrete are shown in Table. 2 and designed compressive strength of concrete was 600 kgf/cm^2. Yield strength of slab reinforcement with nominal diameter of 10 mm was 3261 kgf/cm^2.

2.2 LOADING METHOD

The elevation view of test setup and the plan of gravity loading are shown in Fig. 2 and Fig. 3, respectively. Lateral and gravity loads were applied by two hydraulic actuators attached to the top and the bottom of the columns and by a center holed jacks, respectively. Lateral and gravity loads were applied to the specimens; FPS01, FPS02 and FPS03, while only gravity load was applied to the specimen; FPS04.

Lateral cyclic loading was applied by the following schedule in principle, 2 cycles at $\pm$1/400 rad., $\pm$ 1/200 rad., $\pm$1/100 rad., $\pm$1/50 rad., respectively and a monotonic loading until failure occurred.

The vertical force was applied to eight loading points of the slab separated 52 cm from column faces so that the stress condition in the slab near the column might be similar to that in the prototype buildings by pulling downward with the whiffletree system, and the reaction was subjected to the column base. During the tests of FPS01, FPS02 and FPS03, the vertical jacking force was continuously adjusted to maintain the specified average gravity shear stress; τ v at the connection. FPS01 and FPS03 were given gravity load equivalent to the average shear stress; τ v of 5 kgf/cm^2 at their critical sections which is located at a distance of half of the slab thickness from column faces, and FPS02 was given 10 kgf/cm^2. In the ordinary structural design, the average shear stress at their critical sections by gravity load is about 5 kgf/cm^2. Therefore, the gravity load was 4.88 tf according to τ v of 5 kgf/cm^2 in the cases of FPS01 and FPS03, and 9.75 tf according to τ v of 10 kgf/cm^2 in the case of FPS02.

The gravity load only was applied to FPS04 by a monotonic loading until failure occurred in order to investigate the strength for shear transfer only.

3. TEST RESULTS

3.1 CRACK PATTERNS

The final crack patterns of all specimens are shown in Fig. 4.

The initial crack of FPS04 in which was given only gravity load was observed in the connection of the column and the top surface of the slab. According to the increase of the vertical load, the cracks diagonally developed toward all corners of the slab. After the cracks reached the corner of slab, the circular cracks that connected each vertical loading point were observed in the bottom surface of the slab. Punching shear failure occurred finally.

In the case of FPS01 and FPS03, no cracks were observed when the gravity load of 4.88 tf was applied. The initial cracks were observed in the connection of the column and the top surface of the slab when a deflection angle; R = δ / h, where δ : lateral deflection, h: story height was about 1/650 rad.. The cracks of FPS03 then tended to be developed to the all corners of the slab, but in the case of FPS01 to the free edges of the slab. Although the crack patterns of the bottom surface of the slab were almost same as the top surface, the cracks of the top surface preceded those of the bottom surface in the cases of the both specimens. In the case of FPS01, the punching failure occurred finally in the slab near the column after yielding of all slab reinforcing bars parallel to the lateral load direction. In the case of FPS03, after the crushing failure at the bottom face of the slab near the column occurred, the punching failure occurred in these locations.

In the case of FPS02, when the gravity load of 9.75 tf was applied, the diagonal and orthogonal cracks to the lateral load direction initiated in the slab–column connection. These cracks of the top surface of the slab developed and the new cracks occurred by the application of the lateral load. After the initial crack was observed at the connection of the column and the bottom surface of the slab, new cracks were not observed until the second cycle of +1/100 rad..

3.2 LOAD–DEFLECTION RELATIONSHIPS

The load–deflection relationships of all specimens are shown in Fig. 5. In the early stage of the lateral loading, FPS01 and FPS03 showed almost the same stiffness, but FPS02 to which the higher gravity load was applied showed lower stiffness.

FPS01 reached the maximum strength in R = +1/50 rad. and the punching shear failure occurred in R = +1/23 rad..

In the case of FPS02, after the maximum strength in R= –1/69 rad., the strength deterioration was not occurred and the loading came to an end in R=–1/17 rad..

In the case of FPS03, after reaching the maximum strength in R = +1/32 rad., the crushing failure at the bottom face of the slab near the column occurred and punching shear failure occurred in R=+1/22 rad., with the sudden strength deterioration.

In the case of FPS04 that was given only gravity load, the decline of stiffness was observed in τ v = 7.5 kgf/cm^2, but the initial crack was observed in τ v = 8.4 kgf/cm^2. In τ v = 11.2 kgf/cm^2, the slab deflection started to increase suddenly with the apparent decline of stiffness. The specimen reached the maximum strength of 18.24 tf (τ v = 18.7 kgf/cm^2) in R = 1/50 rad. and then failed in punching shear in R = 1/44 rad..

Shown in Fig. 6 are the equivalent viscous damping values; Heq – deflection angle; R= δ / h relationships of FPS01, FPS02 and FPS03. In the first cycle of R = $\pm$1/200 rad., Heq value for FPS01 is 11.5%, FPS03 9.3%. In the first cycle of R = $\pm$1/100 rad., Heq value is 13.6% for FPS01 and 10.0% for FPS03. The hysteresis loops of FPS01 and FPS03 are slip–typed and thin until R = $\pm$1/100 rad. in FPS01 and R = $\pm$1/50 rad. in FPS03. The hysteresis loop of FPS02 applied high gravity load is spindle shaped

and fatter than other specimens. Heq value is 13.7% in the first cycle of R=±1/200 rad. and 17.5% in the first cycle of R = ± 1/100 rad.. These values increase with decreasing slab reinforcement ratios and increasing the gravity load levels. Hysteretic loop of FPS02 did not exhibit the pinching associated with the shear deterioration of the energy dissipation mechanism.

In the case of FPS02 , it is considered that the high gravity load, which caused excessive slab deflection upward and made moment redistribution unaffected, prevented the bottom reinforcement of slab from reaching the yield stress. Therefore, the hysteretic behavior of a moment type of energy dissipation mechanism for FPS02 can be explained from the fact that the punching shear capacity of the connection was left in reserve because ultimate moment transferred in the slab–column connection became below the retaining capacity of the specimen.

4. DISCUSSION ABOUT TEST RESULTS

4.1 ULTIMATE STRENGTH

When flat plate construction is subjected to simultaneously applied gravity and lateral loads caused by earthquakes or winds, its slab–column connections are stressed in Fig. 7. The shear force; V, caused by the gravity load and the moment; M, caused by the lateral load are balanced by flexure, shear and torsion of the slab sections surrounding the column. A brittle punching shear failure occurs at the slab–column connections unless a yield line mechanism develops first in the flat plate.

For connections transferring both the moment; M, and the shear; V, A. I. J. (Architectural Institute of Japan) proposed the following relationship for the criterion of punching shear strength.

$$V/Vo + M/Mo = 1 \qquad \text{----------} (1)$$

where,

Vo : Predicted shear strength for shear transfer only

$$Vo = 2\tau u (c_1 + c_2 + 2d) d \qquad \text{----------} (2)$$

$$\tau u = 1.06 \sqrt{Fc} \qquad \text{----------} (3)$$

Mo : Predicted moment capacity for moment transfer only

$$Mo = Mf + Ms + Mt \qquad \text{----------} (4)$$

Mf : Flexural strength at the critical section

$$Mf = 0.9 \cdot at \cdot \sigma y \cdot dt (c_2 + d) / st + 0.9 \cdot at \cdot \sigma y \cdot db (c_2 + d) / sb \qquad \text{-----} (5)$$

Ms : Moment transferred by eccentricity of shear at the critical section

$$Ms = \tau u (c_1 + d) d (c_2 + d) \qquad \text{----------} (6)$$

Mt : Torsional moment at the critical section

$$Mt = 2\tau tu (d^2 / 2) (c_1 + d - d/3) \qquad \text{----------} (7)$$

$$\tau tu = 6\tau u \qquad \text{----------} (8)$$

Each symbol in above equation is shown in "**NOTATION**"

Shown in Table. 3 are the ultimate strength of each test specimen and the punching shear strength calculated by Eq. (2) and Eq (4) of the A. I. J. code and the flexural strength expressed in the following.

The flexural strength was calculated by the assumption that yield lines shown in Fig. 9 were formed.

Test results are compared in Fig. 8 with the design expression proposed by the A. I. J. code. In Fig. 8, ordinates are the ratios of the ultimate shear in tests; Vu, to the calculated shear strength for shear transfer only; Vo. Abscissas are the ratios of the ultimate moment in tests; Mu, to the calculated moment capacity for moment transfer only; Mo. The line in the figure represents the criterion of strength predicted by Eq. (1) of the A. I. J. code for the connections transferring both shear and moment.

For FPS01, FPS02 and FPS04 with lower slab reinforcement ratios, the measured strength is smaller than that calculated according to the A. I. J. code. This is because the ultimate strength was governed by the yield of slab reinforcement prior to the final punching shear failure.

For FPS03 with higher slab reinforcement ratio, of which the ultimate strength was governed by the punching shear failure, the measured strength is 30% greater than that calculated according to the A. I. J. code. This shows that the ultimate strength of slab–column connections transferring moment and shear can be predicted using Eq. (1) somewhat conservatively in the case of using high strength concrete.

The flexural strength of FPS01 and FPS04 calculated neglecting the strain hardening of the slab reinforcement and the membrane action in the plane of slab was 31% and 52% smaller than the ultimate strength measured in these tests, respectively. Ref. 6) reported that the increased flexural strength of the slab was due to membrane action and was increasing linearly with (δ + jd) / jd, where δ is the center deflection of the slab and jd is the flexural moment arm as shown in Fig. 10. P_{ult} and P_{flex} in Fig. 10 represent the ultimate capacity in tests and the calculated flexural capacity of the specimens based on undeformed geometry, respectively. From the fact that vertical deflection of the slab was significant in the case of FPS01 and FPS04, it is considered that the membrane action in the plane of the slab was likely to have contributed to the strength.

In the case of FPS02, the bottom reinforcement in the slab did not yield due to the higher gravity load, with the results that the ultimate strength in this test was smaller than the flexural strength calculated on the assumption that the yield lines shown in Fig. 9(a) were formed.

4.2 EFFECTIVE SLAB WIDTH WITH RESPECT TO STIFFNESS

In the case of FPS01, FPS02 and FPS03 subjected to lateral loads, effective slab width coefficients α are calculated from the following Eq. (9), where K and Ke represent the secant modulus obtained from test results and the elastic modulus calculated on the assumption that full slab width is effective to stiffness, respectively.

i.e.; $\alpha = K / Ke$ ---------- (9)

Therefore, the effective slab width with respect to stiffness; Be is the full slab width; B multiplied by α.

i.e.; $Be = \alpha B$ ---------- (10)

Ke was calculated from the analysis of a cruciform frame based on the assumption that the slab can be idealized by the line element having rigid zone in the position of column.

Effective slab width; Be – deflection angle; R relationships are shown in Fig. 11. The effective slab

width; Be for FPS01, FPS02 and FPS03 was 8–15% of the full slab width; B in R=1/200 rad. and 5–11% in R=1/100 rad. as shown as Fig. 11. The effective slab width; Be of three specimens became smaller with increasing lateral deflection. Although Be of FPS01 was not almost different from the value of FPS03 with high reinforcement ratio until R = 1/400 rad., Be of FPS01 became smaller than the value of FPS03 after R = 1/200 rad.. Be of FPS02 applied high gravity load was smallest continually among three specimens. This showed that the effective slab width beyond the elastic region was dependent on the slab reinforcement ratios and the gravity load levels.

However, Fig. 12[4)] shows the effective widths reported by various researchers for slab–column systems using the isotropic elastic plate bending theory. None of the elastic theory can be regarded as satisfactory in their prediction of the effective slab width in these tests.

5. CONCLUDING REMARKS

Seismic tests of slab–column connections of flat plate construction using high strength concrete were carried out and the conclusions were as follows:

1) In the case that the measured strength of specimens was smaller than values predicted by the A. I. J. code, the failure mode of the specimens was flexural failure. However, in the case that the measured strength was greater than those values, the failure mode was punching shear failure. Therefore, the failure mode of flat plate construction using high strength concrete can be predicted by Eq. (1) of the A. I. J. code.
2) The specimen; FPS03, of which ultimate strength was governed by punching shear failure, showed that the ultimate strength of slab–column connections transferring moment and shear can be predicted using Eq. (1) somewhat conservatively in using high strength concrete
3) The hysteretic behavior of connections changed from a shear to a moment type of energy dissipation mechanism with decreasing slab reinforcement ratios and increasing the gravity load levels.
4) These tests showed that the effective slab width beyond the elastic region was dependent on the slab reinforcement ratios and the gravity load levels.

   None of the elastic theory can be regarded as satisfactory in the prediction of the slab effective width in these tests. This shows that the nonlinear model to allow for the reduced stiffness of laterally loaded slab–column system should be proposed.

ACKNOWLEDGMENTS

The tests were achieved under a research committee for developing super high–rise buildings of flat slab construction (Director is Dr. Kanoh, Y., Professor of Meiji University), as a part of New RC projects. The authors are grateful to their cooperation.

REFERENCES

1) Kanoh, Y. and Yoshizaki, S., "Test on Slab–Column Connections under Repeated Lateral Load (Part 1) "Journal of Structural and Construction Engineering , No. 288, pp. 39–47, AIJ, Feb. 1980. (in Japanese)
2) Kanoh, Y. and Yoshizaki, S., "Test on Slab–Column Connections Transferring Shear and Moment (Part 2)" Journal of Structural and Construction Engineering , No. 292, pp. 31–39, AIJ, Jun. 1980. (in Japanese)
3) Kanoh, Y. and Yoshizaki, S., "Strength of Slab–Column Connections Transferring Shear and Moment (Part 4)" Journal of Structural and Construction Engineering , No. 309, pp. 29–40, AIJ, Nov. 1981. (in Japanese)
4) "AIJ Standard for Structural Calculation of Reinforced Concrete Structures" Architectural Institute of Japan., 1988. (in Japanese)
5) N. M Hawkins., "Seismic Response Constraints for Slab Systems" Proceedings of Workshop on Earthquake Resistant Reinforced Concrete Building Construction, pp. 1253–1275, University of California, Berkeley, July 1977.
6) Scott D. B Alexander and Sidney H. Simmonds., "Test of Column–Flat Plate Connections" ACI Structural Journal, Vol. 89, pp. 495–502, Sept – Oct. 1992.
7) Long, A. E., and Kirk, D. W., "Lateral Load Stiffness of Slab–Column Structure" Reinforced Concrete Structures Subjected to Wind and Earthquake Force, SP–63, pp. 197–220, American Concrete Institute, Detroit, 1980.
8) David A, Pecknold., "Slab Effective Width for Equivalent Frame Analysis" ACI Journal, pp. 135–137, April 1975.

NOTATION

at = area of tensile reinforcement

Be = effective slab width with respect to stiffness

B = full slab width

c = width of face of isotropic column

c_1 = width of longitudinal face of column

c_2 = width of transverse face of column

d = effective depth to centroid of tensile reinforcement

db = effective depth to centroid of bottom reinforcement for positive moment

dt = effective depth to centroid of top reinforcement for negative moment

Fc = concrete cylinder compressive strength

K = ratio of secant modulus obtained from test results

Ke = elastic modulus calculated on the assumption that full slab width is effective

Mo = predicted moment capacity for moment transfer only

Mf = flexural strength at the critical section

Ms = moment transferred by eccentricity of shear at the critical section

Mt = torsional moment at the critical section

Mu = ultimate moment in test

sb = spacing of bottom reinforcement for positive moment

st = spacing of top reinforcement for negative moment

Vo = predicted shear strength for shear transfer only

Vu = ultimate shear in test

α = effective slab width coefficient

σ y = yield stress of reinforcement

τ u = ultimate vertical shear stress

τ tu = ultimate torsional shear stress

TABLE.1 Test Parameters

Specimen	Loading Method [1*]	Slab Reinforcement			τ_v (kgf/cm²) [2*]
		Column Strip		Middle Strip (Top, Bottom)	
		Top	Bottom		
FPS01	H + V	D10@150	D10@300	D10@300	5.0
FPS02	H + V	D10@150	D10@300	D10@300	10.0
FPS03	H + V	D10@80	D10@80	D10@160	5.0
FPS04	V	D10@150	D10@300	D10@300	-

(NOTE) [1*]: H is Lateral Loading and V is Gravity Loading.
[2*]: Average Shear Stress at Critical Section by Gravity Load

TABLE.2 Concrete Properties

Specimen	Compressive Stress (kgf/cm²)	Young's Modulus ($\times 10^5$ kgf/cm²)	Splitting Stress (kgf/cm²)
FPS01, 02, 03	731	3.98	50.8
FPS04	631	4.02	47.0

TABLE.3 Ultimate Strength

Speci-men	Test Results			A.I.J. Formula (Eq.(1))					Flexural Strength		Mode of Failure [3*]
	Mu(tm)	Vu(tf)	${}_tV_{my}$(tf) [1*]	Mo(tm)	Vo(tf)	Mu/Mo	Vu/Vo	Mu/Mo+Vu/Vo	M_t(tm)	${}_cV_{my}$(tf) [2*]	
FPS01	4.38	4.88	—	5.81	28.0	0.75	0.17	0.92	3.33	-	F→S
FPS02	2.82	9.75	—	5.81	28.0	0.49	0.35	0.84	3.33	-	F^+
FPS03	7.40	4.88	—	6.56	28.0	1.13	0.17	1.30	8.89	-	S
FPS04	—	18.24	12.19	—	25.9	—	0.70	0.70	—	12.02	F→S

(NOTE) [1*]: ${}_tV_{my}$ = Measured vertical load when yield lines shown in Fig.9(C) were formed in R=1/400 rad..
$M_t = 2M_y \cdot l/l_F$: $M_y = 0.9 \cdot a_t \cdot \sigma_y \cdot d$
[2*]: ${}_cV_{my}$ = Vertical load calculated from the assumption that the yield line shown in Fig.9(B) were formed.
[3*]:Mode of Failure
F→S= After the ultimate strenghs were governed by the yield of slab reinforcement, punching shear failure occured finally.
F^+ = After the ultimate strenghs were governed by the yield of slab reinforcement, the loading came to an end in R=-1/17rad..
S = Punching shear failure

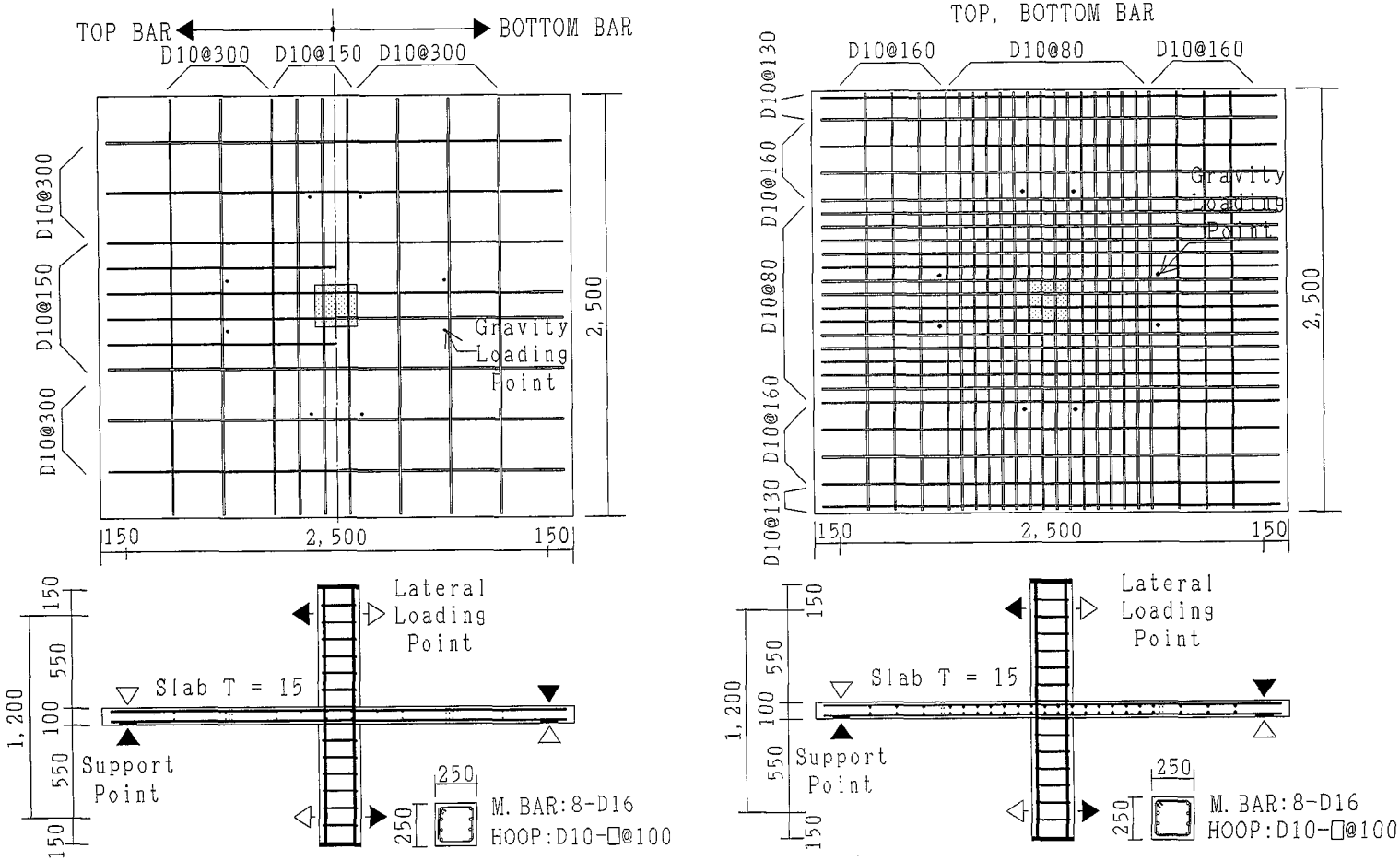

(A) FPS01, FPS02, FPS04

(B) FPS03

Fig. 1 Test Specimens

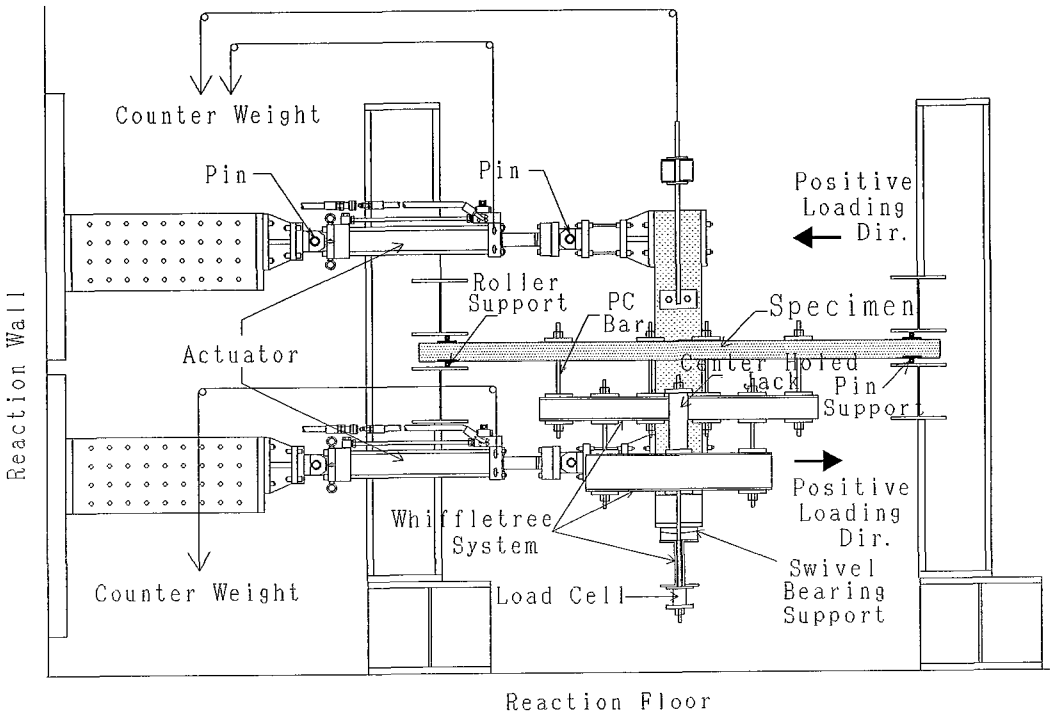

Fig. 2 Elevation View of Test Setup

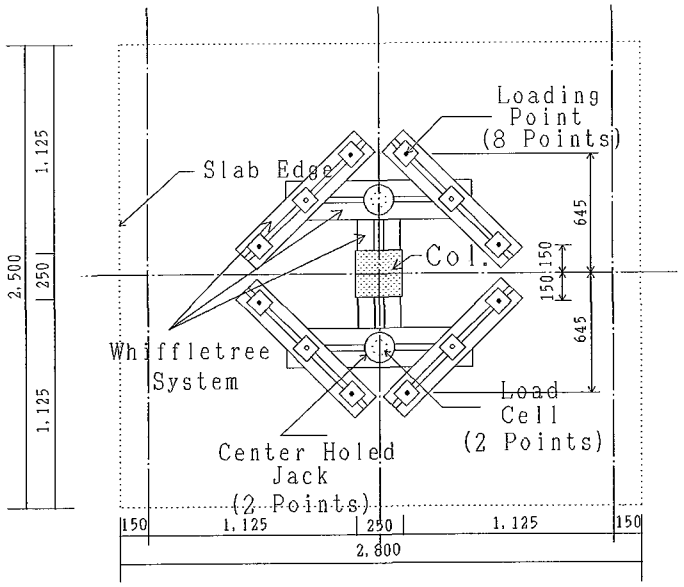

Fig. 3 Plan of Gravity Loading System

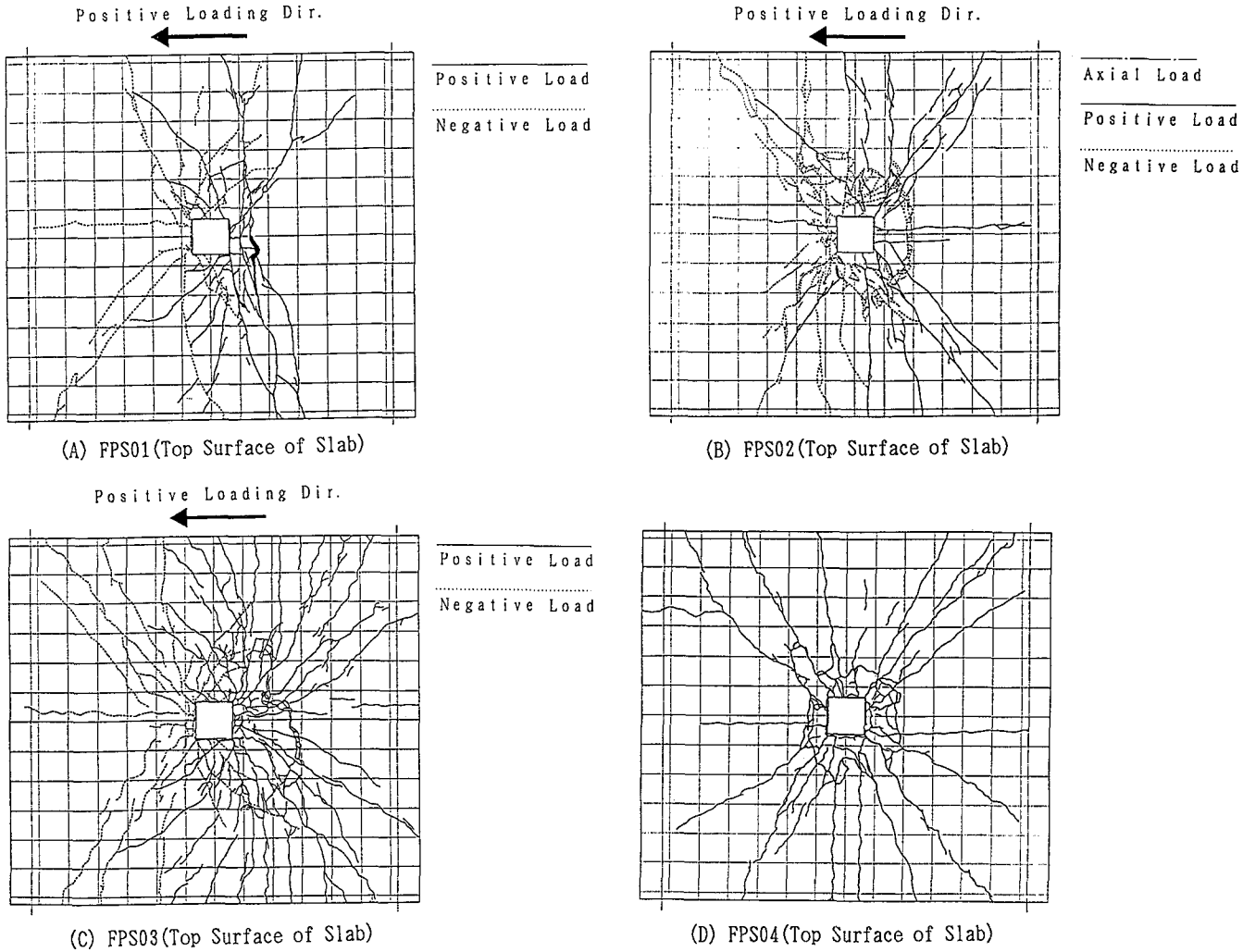

(A) FPS01(Top Surface of Slab)

(B) FPS02(Top Surface of Slab)

(C) FPS03(Top Surface of Slab)

(D) FPS04(Top Surface of Slab)

Fig. 4 Final Crack Patterns

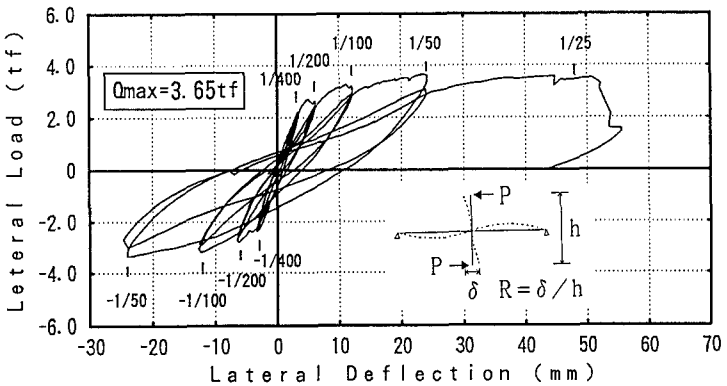

(A) Specimen FPS01

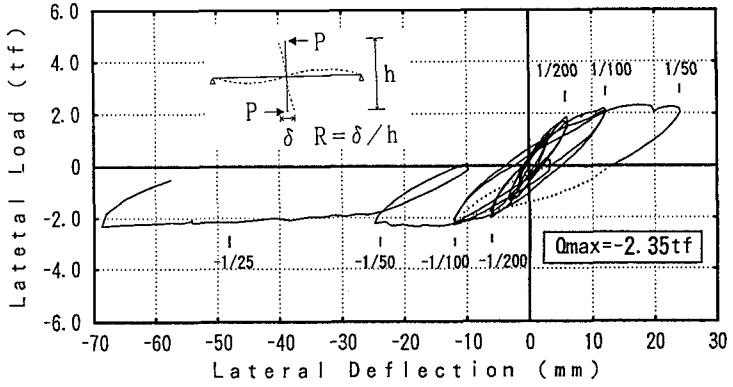

(B) Specimen FPS02

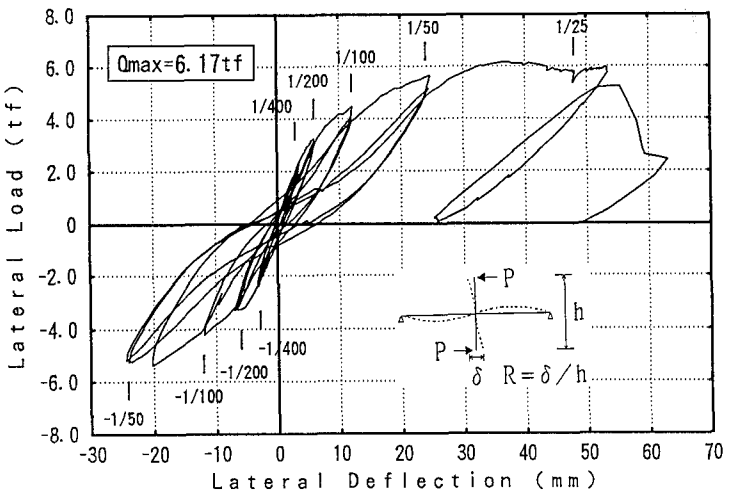

(C) Specimen FPS03

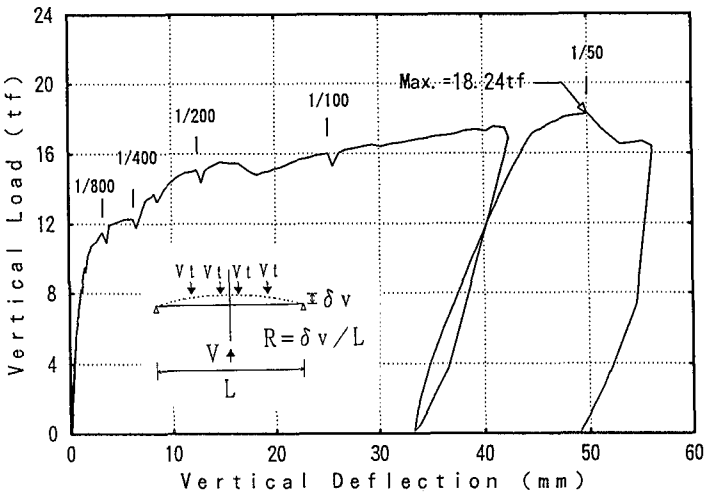

(D) Specimen FPS04

Fig. 5 Load-Deflection Relationships

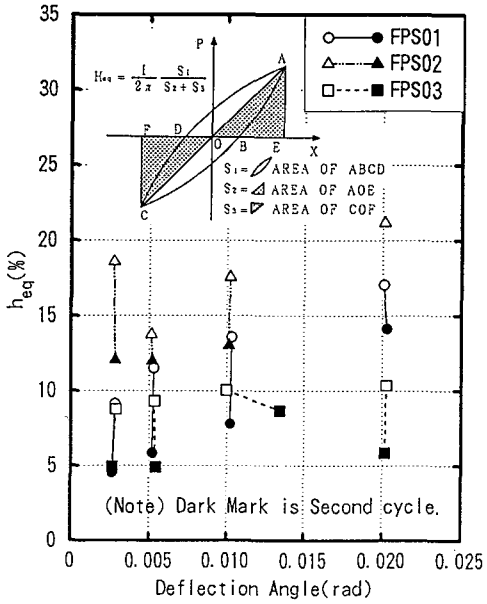

Fig. 6 h_{eq} - Deflection Angle Relationships

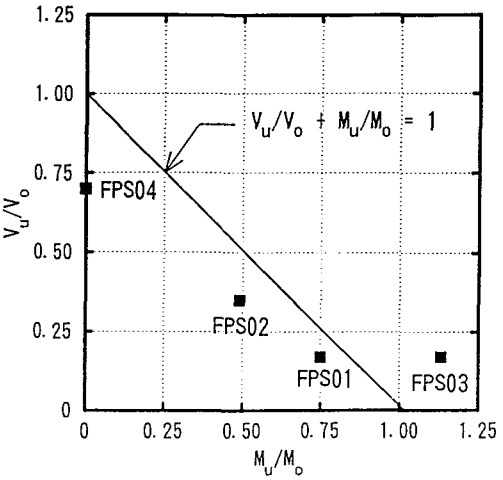

Fig. 8 V_u/V_o - M_u/M_o Relationships

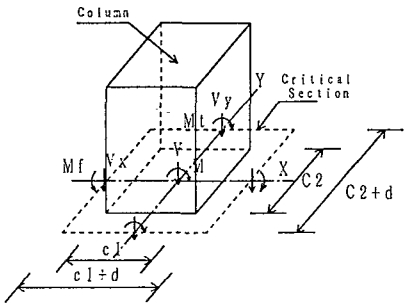

Fig. 7 Forces acting at the critical section

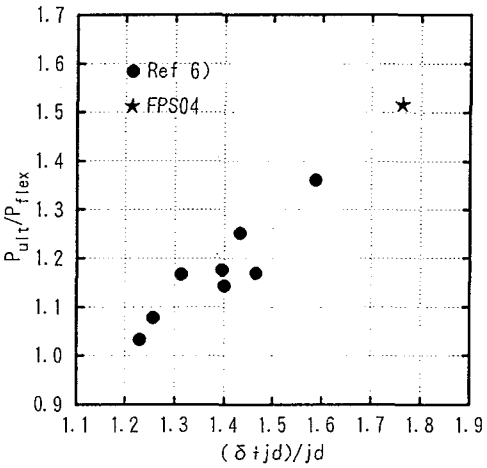

Fig. 10 Effect of Deflection on Flexural Strength[6)]

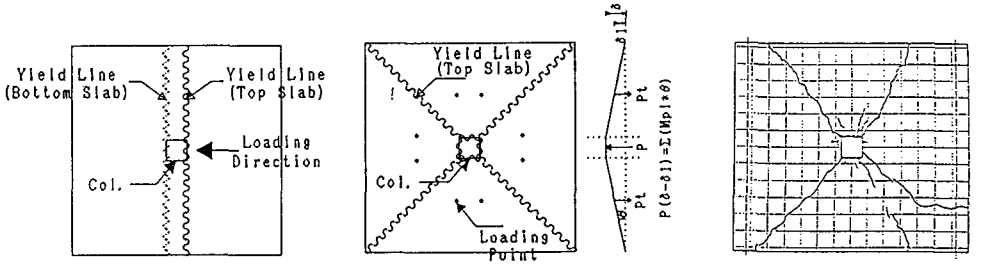

(A) Assumpted Yield Lines of FPS01, FPS02, FPS03

(B) Assumpted Yield Lines of FPS04

(C) Actual Yield Lines of FPS04 (R=1/400 rad.)

Fig. 9 Yield Lines

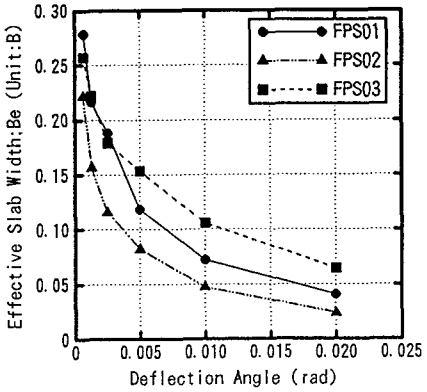

Fig. 11 Effective Slab Width - Deflection Angle Relationships

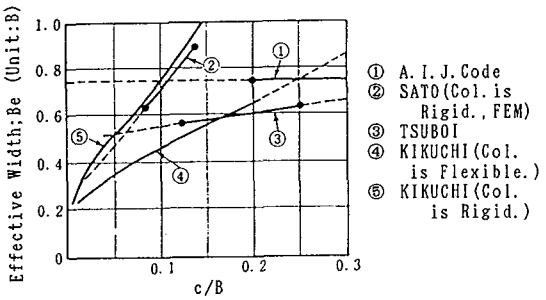

Fig. 12 Effective Width;Be for Equivalent Frame Subjected to Lateral Load[4)]